Sensors and Materials, Vol. 34, No. 11 (2022) 4113–4126
MYU Tokyo

S & M 3100

Characteristics of Magnetic Resonance Wireless Power Transfer Across Gap Distance Using Metallic Wire Coils

Arvanida Feizal Permana, Adhe Martiya,
C. Bambang Dwi Kuncoro, and Yean-Der Kuan*

Department of Refrigeration, Air Conditioning and Energy Engineering,
National Chin-Yi University of Technology, Taichung 41170, Taiwan

(Received May 24, 2022; accepted November 8, 2022)

Keywords: magnetic resonance, wireless power transfer, coil materials

Significant progress has been made in the area of wireless power transfer (WPT) during the last few years. Large air gaps can now be crossed using power, according to recent research. WPT was used at the small scale, such as in mobile phones, before its proposal for use in large-scale electric equipment such as electric vehicles. Furthermore, it is planned that all electrical cords will be replaced with WPT units. Electric resonance coupling enables high-efficiency power transmission across large air gaps. This has been used in communication technology antennas and resonators and is closely connected to electromagnetic induction. In contrast to coupled mode theory, equivalent circuits—a topology more familiar to electrical engineers—are used in this study to investigate power transfer phenomena and technologies. By combining various combinations of coils for the transmitter (Tx) and receiver (Rx), it should be possible to increase the gap between the coils. Therefore, a pair of Tx and Rx coils is analyzed by computer simulation and lab experiments to measure the voltage and current received by the Rx module. The result for a 14 cm gap between the coils shows that the designed module can transmit power wirelessly over a medium-distance gap.

1. Introduction

Numerous outstanding advances have been achieved in the area of wireless power transfer (WPT) and have drawn much interest. Recent improvements in WPT show that it is possible to cross increasingly large air distances with excellent efficiency.(1) All electrical equipment can benefit from a direct feed WPT approach. As a consequence, automated WPT is replacing cables in homes. This technology may be used both inside and outside the home. In a parking area, WPT can be used to charge electric bicycles and electric vehicles.(2) It is critical to accomplish high-efficiency power transfer across very large air gap distances to make this type of system possible. High efficiency is still not possible, despite the fact that microwave power transfer or laser power transfer can span air distances greater than a few kilometers. The shape and size of the coils also become variables in determining the allowable air gaps between the transmitter (Tx) and receiver (Rx) modules.(3)

*Corresponding author: e-mail: ydkuan@ncut.edu.tw
https://doi.org/10.18494/SAM4131

ISSN 0914-4935

The earliest account of wireless data and power transfer based on the magnetic coupling between a pair of coils dates back to Tesla's laboratory tests in 1914.[4] Tesla created a small air gap across which electrical energy could be transmitted without any physical contact using the mutual induction principle between two coils. The results of his experiment supported Faraday's discovery of magnetic induction more than 180 years earlier.

According to a recent survey, reciprocal induction coupling is the most popular approach of WPT technology for a variety of applications.[5-9] Unfortunately, this approach can only be used for applications requiring close-range operation. The other WPT approach of magnetic resonant coupling was theoretically and empirically validated in 2007 by MIT researchers.[10,11] The outcomes of their experiments demonstrated the potential for WPT technology to advance applications for midrange operations.

We propose a technology based on electromagnetic resonant coupling by optimizing the capacitances formed in series or parallel in the Tx and Rx coils. This two-coil system can be varied in size, which can increase the transmission distance. A simulation is performed in which ANSYS is used to design the coil and analyze the magnetic flux for power transfer. From this simulation, we can determine the most suitable material for the coil design and create the coil. We can also determine the maximum transmission distance from the Tx coil to the Rx coil. An experiment to measure the gap and angle between the Tx and Rx coils is then performed for verification.

2. Materials and Methods

2.1 Wireless power transfer theory

Electromagnetic induction coupling is the foundation of the most popular WPT technology. This idea is based on Faraday's induction law and Ampère's circuital law, two fundamental electromagnetic field rules.[12] The Maxwell equation incorporates these rules. The relationship between the magnetic field and the electric current that it creates is introduced using Ampère's circuital law. The total current I that flows across the surface encompassed by a curve is proportional to the integral along the line of the magnetic field surrounding the closed curve according to the Kelvin–Stokes theorem:

$$\oint B.dl = \mu_0 \oint Jds = \mu_0 \Sigma I, \tag{1}$$

where μ_0 is the constant for the magnetic field and J is the free current density. The magnetic flux density is acquired as[13]

$$\oint B.dl = 2\pi r.B = \mu_0 i, \tag{2}$$

$$B = \frac{\mu_0 .i}{2\pi r}. \tag{3}$$

Faraday demonstrated electromagnetic induction in his experiments. Any closed conducting loop will experience a time-varying magnetic flux as a result of the electromotive force (emf) from the coil. Faraday's law describes the emf as

$$emf = -N\frac{d\Phi}{dt}, \tag{4}$$

where Φ is the coil's magnetic flux. An emf voltage is induced in the second coil as a result of any variation in the magnetic flux flowing through the first coil. The following is an expression for the magnetic flux passing through the first coil:

$$\Phi = BA.\cos\theta. \tag{5}$$

Equation (5) states that the magnetic flux density must be perpendicular to the surface cross section from the coil for the magnetic flux through the coil to reach its maximum value. Using the Biot law, Savart essentially described the relationship between the magnetic field source (current) and the magnetic field itself as[14]

$$B = \frac{\mu_0 NiR^2}{2\left(R^2 + Z^2\right)^{\frac{3}{2}}}, \tag{6}$$

where Z is the distance between any two points of the coil. I is therefore the amount of current flowing through the coil. Comparing Eqs. (4)–(6), we can state the following:

$$emf = \alpha.i\,. \tag{7}$$

The current flowing through the Tx coil has a direct impact on the voltage induced at the Rx coil. A higher voltage will be induced in the Rx coil when the current in the Tx coil increases significantly.

2.2 Magnetic resonance coupling

Magnetic resonance occurs when a capacitor is included, making inductor impedances that cancel out with the capacitance in magnetic resonant coupling.[15] This occurs at a specific frequency known as the resonant frequency, given by

$$\omega = \frac{1}{\sqrt{LC}}. \tag{8}$$

The distance over which power may be transferred wirelessly increases significantly when the impedances cancel out since there is no voltage drop across L and the only voltage drop on the receiving side is caused by the inductor's parasitic resistance. The greatest power given to the load by magnetic resonance occurs at a specific distance. Moving the coils closer together from this distance reduces the power sent to the load.[16] Equation (9) gives the amount of power applied to the load:

$$P_{out} = \frac{Vin^2 \left(\omega M\right)^2 R.L}{\left(Zt.Zr + \left(\omega M\right)^2\right)^2}, \tag{9}$$

where Zt and Zr are the Tx and Rx impedances, respectively, M is the mutual inductance, and $R.L$ is the load resistance. This equation clearly illustrates how the input voltage, the coupling factor of the two inductors, and their respective impedances all affect the amount of power transferred to the load. Equation (10) describes how M and D are related:

$$M = \frac{\pi \mu_0 nt.nr\left(rt.rr\right)^2}{2D^3}. \tag{10}$$

The numbers of layer turns on the Tx and Rx sides are *nt* and *nr*, respectively. The radii of the Tx and Rx coils are *rt* and *rr*, respectively, where D is the air gap distance between the coils. The inverse cube relationship between mutual inductance and distance may be seen in this equation. The power dramatically drops with increasing distance between the Tx and Rx coils. The inductor coils are designed using Eq. (10). The inductance is influenced by the wire diameter, the cross-sectional area of the antenna, the number of layer turns, and the number of spacing turns.

3. Design and Simulations

3.1 Proposed design

The electromagnetic connection serves as the foundation for the architecture of the proposed module. The switching and oscillator circuits, power amplifier circuit, resonator circuit, and Tx coil that produce the resonant frequency make up the basic circuit of the Tx. The secondary circuit of the Rx, in contrast, consists of a front-end resonator circuit, a rectifier and regulator circuit, and an Rx coil, as shown in Fig. 1. By setting the Tx and Rx coils to the same resonant frequency, the Tx delivers power to the loads (such as electrical, electronic, battery-operated, mobile, and other devices) through the Rx. At a maximum distance of 10 cm, the incoming voltage signal is converted into a stable output voltage of 5 V and a peak current of 2 A. Wheeler's formula was approximated to produce the Tx and Rx resonators.

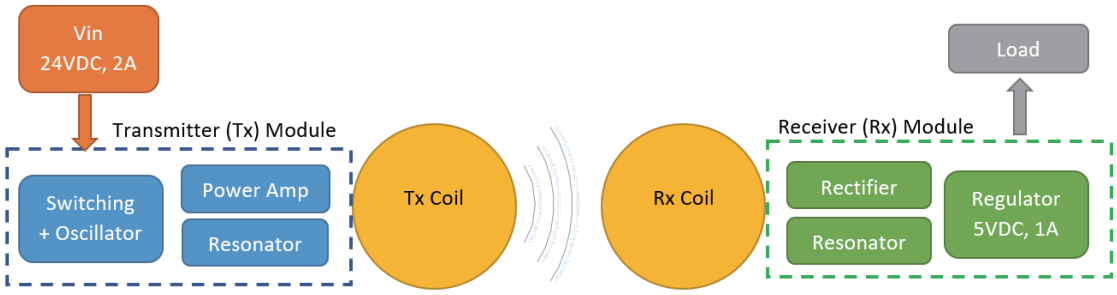

Fig. 1. (Color online) Proposed design of the components for the resonant WPT.

3.2 Coil design

When designing coils for a wireless power charging system, magnetic fields are a crucial consideration. The primary coil, which serves as the driving coil or the Tx coil, the secondary coil, which serves as the Rx coil, and the load must thus receive additional attention during the design stages. In the first stage of the WPT system design, a number of design considerations must be made for each coil to optimize the coupling coefficient between the two coils. The coil shape, wire size and type, number of layer turns, air gap distance between the coils, and amount of magnetic field produced by the two coils are relevant factors.[17] In practice, the WPT system should be implemented with Tx and Rx coils of the same size to produce more effective power transmission. To maximize the current and the magnetic coupling into the Rx coil, it is important that the Tx coil creates a strong magnetic field.

To determine the performance of the proposed wireless power system, the electromagnetic properties of each coil require consideration. A single-layered coil design was adopted to increase the efficiency, the Q-factor, the power handling, and the associated magnetic field produced by the Tx coil. Rosenbaum's modification of Wheeler's formula may be used to measure the self-inductance from a single-layered air core coil:[18]

$$L = 0.002\pi dN2\left[Ln\left(1\pi 2l\,d\right) + \frac{1}{2.303 + 3.213ld + 1.784\left(dl\right)^2} \right]. \tag{11}$$

Before creating a fixed wireless coil, the coil was first designed using ANSYS 3D Maxwell to determine the most suitable material for transmitting the power source from the Tx to the Rx and producing the strongest possible magnetic field so that it radiates the furthest distance and the Rx can receive the power, as shown in Fig. 2.

Based on the simulation results, several materials were used to make a wireless coil before we made the actual coil. In addition to being more time efficient, this approach also provides information about the maximum area of the magnetic flux that can be achieved with the specified design, as shown in Table 1. Magnetic flux values were obtained from copper, aluminum, and stainless steel. From the table, the magnetic flux values for copper, aluminum, and stainless steel are seen to be similar. However, we used copper wire for the Tx and Rx in this

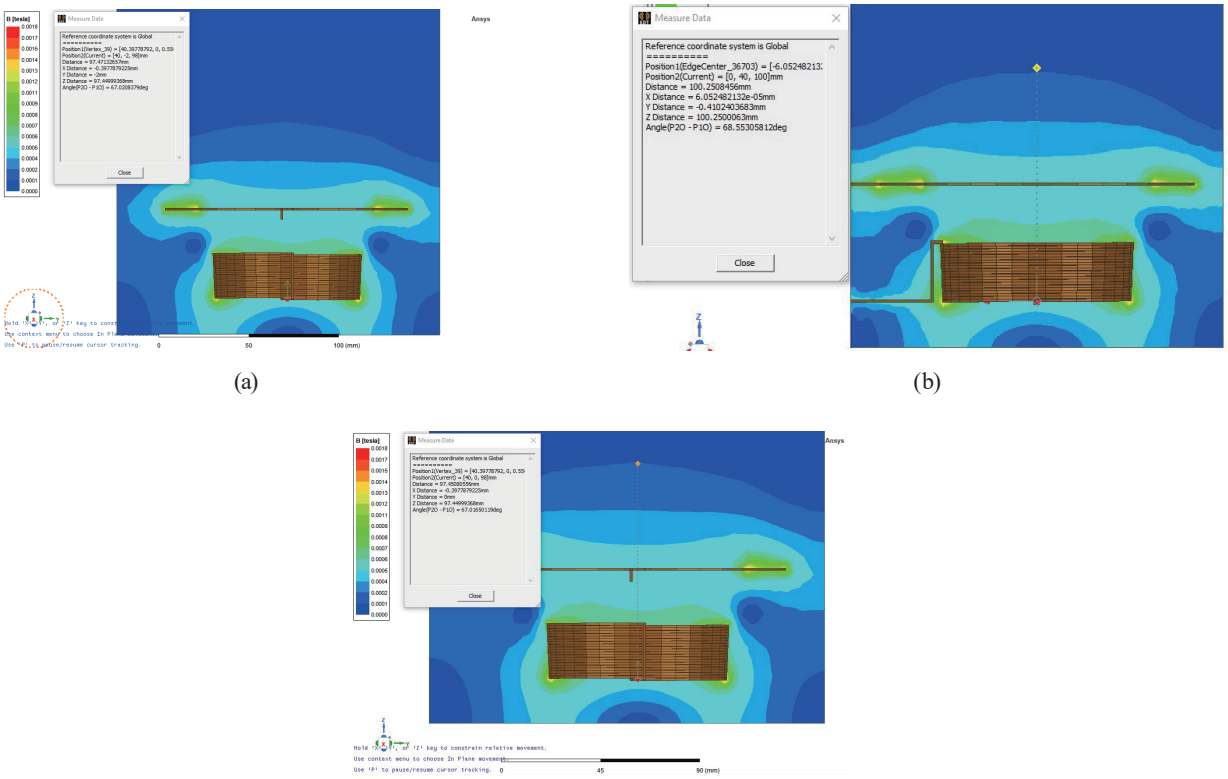

Fig. 2. (Color online) Magnetic field simulation of different material coils: (a) stainless steel, (b) copper and (c) aluminum.

Table 1
Magnetic flux of Tx for different coil materials.

Distance (mm)	Magnetic flux of Tx (Wb)		
	Copper	Aluminum	Stainless steel
35	9.7×10^{-5}	9.695×10^{-5}	9.69×10^{-5}
45	9.1×10^{-5}	9.13×10^{-5}	9.124×10^{-5}
55	8.7×10^{-5}	8.701×10^{-5}	8.704×10^{-5}
65	8.4×10^{-5}	8.411×10^{-5}	8.414×10^{-5}
85	8.1×10^{-5}	8.018×10^{-5}	8.072×10^{-5}
100	7.9×10^{-5}	7.944×10^{-5}	7.946×10^{-5}

study because copper is stronger than aluminum. Although copper expands less than aluminum, both materials have a similar maintenance schedule. Copper has almost twice the current capacity as aluminum, which allows copper coils to be slightly smaller than aluminum coils. Stainless steel is a poor conductor because it has an alloy structure. The average thermal conductivity of copper is 20 times that of stainless steel. In practical terms, copper can transfer heat 20 times faster.

Using Eq. (8), a Tx coil was created with the shape of a single-layered air core coil. It had an inductance of 32.6 H, 7.99 turns, a length of 8.189 mm, and a diameter of 130 mm. Because of its small diameter and ability to transmit a maximum current of 4 A, an enameled AWG 17 wire

was selected. The final manually constructed Tx coil comprised 15 turns and had a 150 mm diameter, a 9.0 mm thickness, and a measured inductance of 93.87 μH. Figure 3 depicts the geometry of the Tx coil.

The Rx coil had a different shape and diameter compared with the Tx coil to enhance the coupling efficiency. The final constructed Rx coil had seven turns, a coil diameter of 200 mm, and a thickness of 7.0 mm. The measured inductance was 40.58 μH. Figure 4 depicts the Rx coil geometry.

3.3 Module design

The proposed architecture in Fig. 1 was used to develop and build the Rx and Tx circuits. The Rx module coil was induced by the magnetic flux produced by the Tx module, allowing the Rx circuit to gather the power transferred. Therefore, the maximum amount of electric power may be transferred through an air gap more effectively using the magnetic resonant technique without the need for a wire connection.[19]

The Tx and Rx coils were driven by the resonator circuit to run at the same operating frequency to transfer power from the Tx to the Rx. The resonant frequency of the WPT system is the same as its operating frequency. Equation (7) may be used to find the resonant frequency.

In this study, the resonant frequency was produced via parallel coupling capacitors. The Tx coil incorporates a parallel capacitor; the Rx coil incorporates another parallel capacitor. When the WPT working frequency is tuned at the resonant frequency or a harmonic resonant frequency, the maximum power can be transmitted from the source power supply into the load through the Tx and Rx coils.

The parallel capacitor has a resonant frequency of 140 kHz. Equation (9) may be used to obtain the capacitance of the parallel capacitor from the definition of the Tx coil inductance given above. The capacitor has a value of 39 nF. Figure 5 depicts how the Tx module is implemented.

The Tx module can operate with a maximum current of 2 A and a 24 V DC input voltage. Figure 6 depicts the implemented Rx module. To operate at the resonant frequency, the Rx module is additionally equipped with a resonator circuit with a 45 nF parallel capacitor. The Rx module includes a rectifier circuit that regulates the output voltage from 5 V up to a maximum current of 2 A.

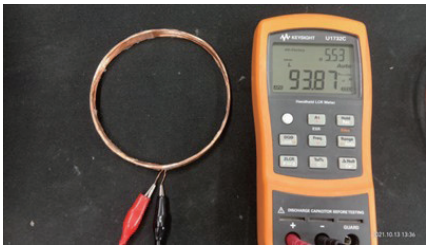

Fig. 3. (Color online) Tx coil geometry for the resonant WPT..

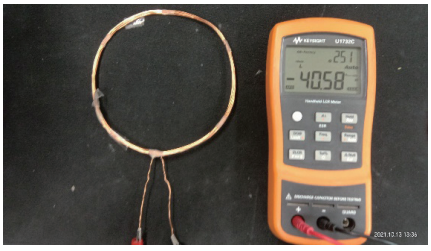

Fig. 4. (Color online) Rx coil geometry for the resonant WPT.

4. Experiments and Results

4.1 Coil simulation using ANSYS

A computer simulation using ANSYS was conducted to simulate the magnetostatic condition of the WPT coils. A researcher can analyze the content to determine the power transfer between the coils. The Tx and Rx coils with specifications based on the proposed design were drawn and built as depicted in Fig. 7(a). The simulation was later run, and a graph of the results is shown in Fig. 7(b).

The simulation result shows that the proposed design of the Tx coil can transfer power to the Rx coil, with peak transfer at a distance of 35 mm and the transfer power decreasing up to a length of 100 mm. This simulation also provided us with the values of the magnetic flux and the inductance between the Tx and Rx coils for distances from 35 to 100 mm, as shown in Table 2.

4.2 Lab module experiment

The Tx and Rx modules were paired with their coils, and an experiment was performed to measure the power transfer from the Tx module and the current received by the Rx module. The Tx module was powered using a DC power supply with a 12 V input. Figure 8 shows the Tx module combined with the coil.

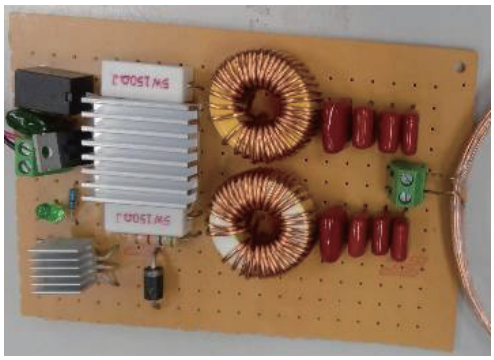

Fig. 5. (Color online) Design of resonant WPT Tx module.

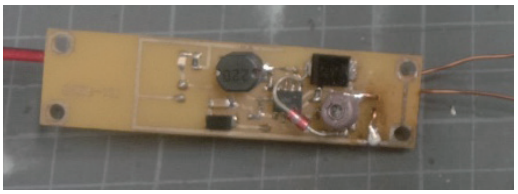

Fig. 6. (Color online) Design of resonant WPT Rx module.

Table 2
Impedance of coil design.

dist (mm)	Matrix1.CplCoef (TX1,RX1)	Matrix1.L(TX1,RX1) (uH)	Matrix1.MagFlux(TX1) (Wb)	Matrix1.MagFlux (RX1) (Wb)
35	0.253604571	10.0831796	9.69×10^{-5}	9.25×10^{-5}
45	0.177844703	7.090870923	9.12×10^{-5}	8.73×10^{-5}
50	0.147677044	5.893452018	8.90×10^{-5}	8.51×10^{-5}
55	0.122372311	4.885322901	8.70×10^{-5}	8.33×10^{-5}
65	0.083684792	3.344481779	8.41×10^{-5}	8.05×10^{-5}
85	0.039131687	1.564027917	8.07×10^{-5}	7.71×10^{-5}
100	0.022193475	0.887206141	7.95×10^{-5}	7.59×10^{-5}

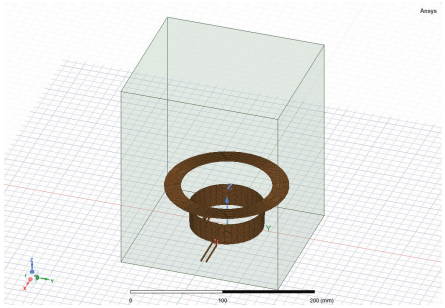

(a)

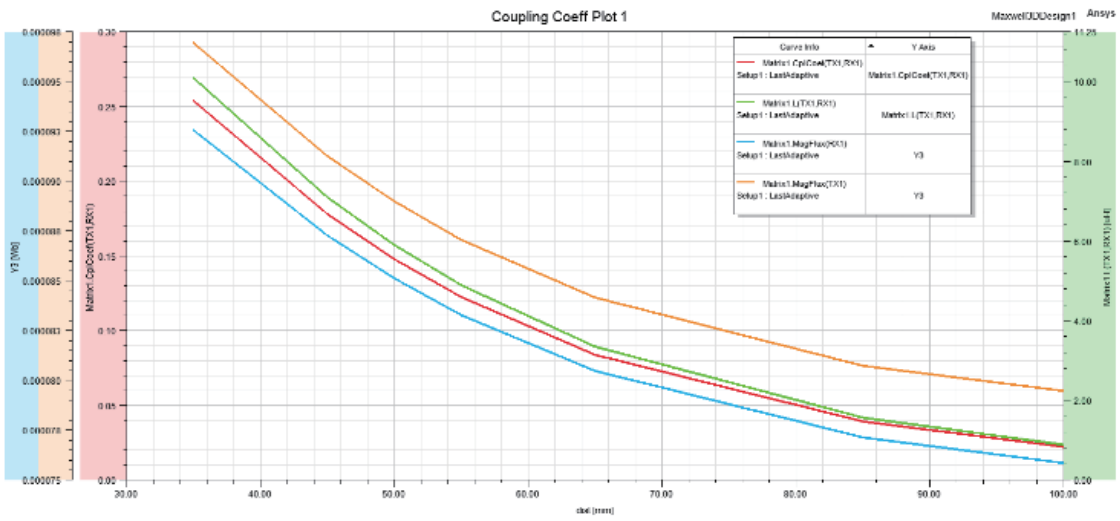

(b)

Fig. 7. (Color online) (a) Coil design simulation and (b) simulation result.

In the Rx module, a battery charger circuit was placed at the load in series with an Lir2032 3.3 V coin battery. The coin battery was paired with the battery charger circuit to show that the Rx module can receive electricity from the Tx module and is sustained by the battery. Figure 9 shows the combined Rx module.

After both the Tx and Rx modules were paired with their peripherals, an experiment was carried out by supplying a DC voltage to the resonant module, which was then fed to the Tx. The Tx coil transmits the power supplied by the resonant module. The Rx coil is positioned perpendicular to the Tx coil by gradually increasing the distance between the Tx and the Rx to determine the maximum distance at which the Tx can transmit to the Rx. A DC electronic load was used to measure the power voltage received by the Rx. The DC electronic load was first set at constant voltages (CVs) of 5 and 3.3 V to obtain the current measured in the Rx circuit. Constant resistances (CRs) of 100 and 1000 Ω were used to analyze the voltage and current characteristics of the modules. Figure 10 shows the experimental setup.

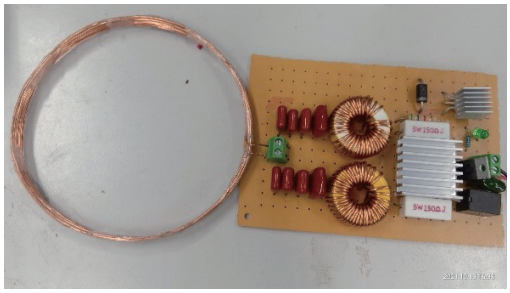

Fig. 8. (Color online) Tx module combined with coil.

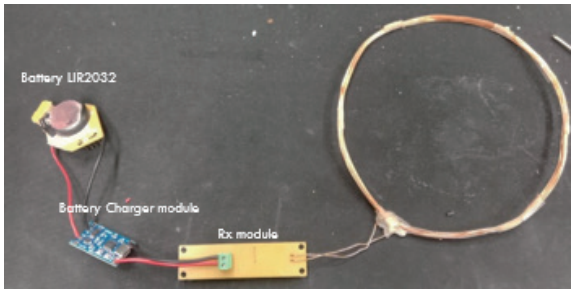

Fig. 9. (Color online) Rx module combined with coil, battery charger, and Lir2032 battery.

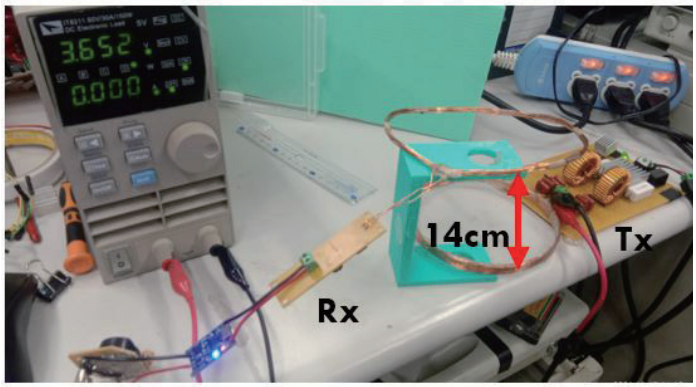

Fig. 10. (Color online) Experiment setup of WPT between Tx and Rx.

4.3 Measurement result

The resonant WPT experiment was performed with the DC electronic load set as CVs of 3.3 and 5 V. The highest current of around 300 mA was obtained when the gap distance was 0 cm for CVs of both 3.3 and 5 V. The voltage then gradually decreased as the gap enlarged. As a result, the current that the Rx module can receive is inversely proportional to the size of the gap distance. The greater the gap between the Tx and the Rx, the smaller the current that can be received by the Rx. The current continuously decreases up to the maximum gap distance of 14 cm. When the gap distance is 15 cm, the Rx module can no longer receive the current, i.e., the measured current is zero. Figure 11 shows the experiment result.

The results obtained for the voltage and current measurement when the DC electronic load was set as CRs of 100 and 1000 Ω are shown in Figs. 12(a) and 12(b), respectively. The measured voltage for the 100 Ω CR drops when the gap reaches 7 cm, which is sooner than that for the CR of 1000 Ω, for which a current is sustained up to a distance of 14 cm. The current measurement adjusts to the same value as the voltage measured by the CR value. This measurement aims to determine the effect of the CR value on the measured current. For the CR setting of 100 Ω, the

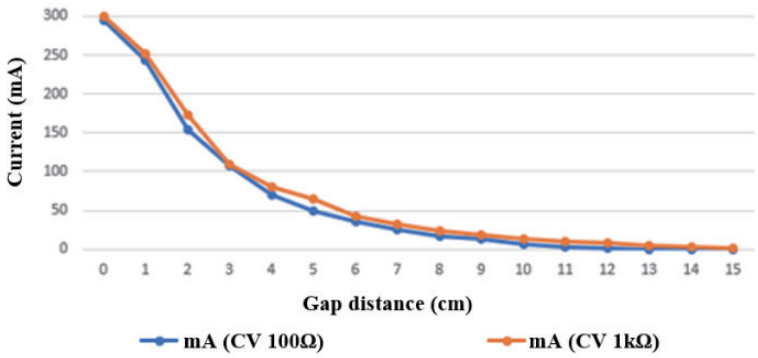

Fig. 11. (Color online) Current measurement result from CV setup.

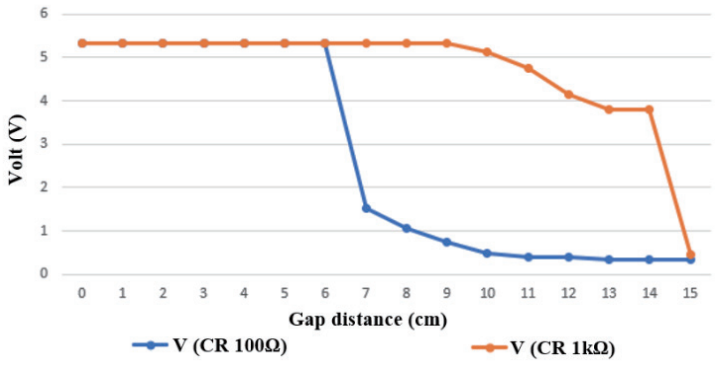

(a)

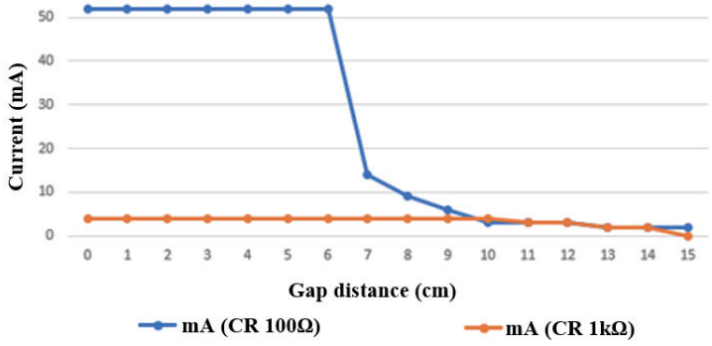

(b)

Fig. 12. (Color online) Measurement results for CR setup: (a) voltage measurement and (b) current measurement.

current measured is constant from a gap distance of 0 to 6 cm and then drops as the gap distance further increases. As the gap distance increases from 7 to 15 cm, the rated current drops from 15 to 5 mA. In contrast, for the CR setting of 1000 Ω, the current tends to be constant at a value of 5 mA from a gap distance of 0 to 12 cm and then drops to 0 mA at a gap distance of 15 cm.

These experiments show that power was successfully transferred between the Tx and Rx modules. The voltage provided is sustainable and sufficient to charge a battery module, which means that it can charge low-voltage sensors and other electronic devices.

5. Conclusion

A technique to maximize the WPT transmission distance was proposed in this study. Several tests and validations were conducted, which demonstrated that the proposed method increases the transmission distance of a WPT system. The experimental findings show that the WPT system developed in this study can transmit data up to a distance of approximately 14 cm and provide a maximum power voltage transfer of 5 V. The current for the load can reach 300 mA at the minimum distance, and a current of 20 mA can be sustained at a distance of 10 cm. The experimental findings also indicate that a WPT system using this technique can transmit electricity. The results show that the magnetic resonance coupling approach increases the transmission distance and the effectiveness of power transfer.

Acknowledgments

This work was supported in part by the Ministry of Science and Technology, Taiwan (number MOST110-2221-E-167 -013 -MY2).

References

1 T. Imura: Proc. 2010 IEEE Int. Symp. Industrial Electronics. (IEEE, 2010) 3664–3669.
2 M. Debbou and F. Colet: Proc. 2016 IEEE PELS Workshop on Emerging Technologies: Wireless Power Transfer (WoW) (IEEE, 2016) 118–122.
3 Y. Yi, U. Buttner, Y. Fan, and I. G. Foulds: Proc. 2013 IEEE Wireless Power Transfer (WPT) (IEEE, 2013) 230–233.
4 B. Zhu, J. Li, W. Hu, and X. Gao: 2015 Int. J. u- and e- Service, Sci. Technol. **8** (2015) 257. https://doi.org/10.14257/ijunesst.2015.8.3.25
5 S. Li and C. C. Mi: IEEE Trans. Emerg. Sel. **3** (2015) 4. https://doi.org/10.1109/JESTPE.2014.2319453
6 J. J. Casanova, Z. N. Low, and J. Lin: IEEE Trans. Ind. Electron. **56** (2009) 3060. https://doi.org/10.1109/TIE.2009.2023633
7 Y. J. Jang, E. S. Suh, and J. W. Kim: IEEE Syst. J. **10** (2016) 495. https://doi.org/10.1109/JSYST.2014.2369485
8 S. Y. Choi, B. W. Gu, S. Y. Jeong, and C. T. Rim: IEEE J. Emerg. Sel. Top. Power Electron. **3** (2015) 18. https://doi.org/10.1109/JESTPE.2014.2343674
9 W. Zhang, S.-C. Wong, C. K. Tse, and Q. Chen: IEEE Trans. Power Electron. **29** (2014) 2979. https://doi.org/10.1109/TPEL.2013.2273364
10 A. Karalis, J. D. Joannopoulos, and M. Soljačić: Ann. Phys. **323** (2008) 34. https://doi.org/10.1016/j.aop.2007.04.017
11 A. Kurs, A. Karalis, R. Moffatt, J. D. Joannopoulos, P. Fisher, and M. Soljacic: Science **317** (2007) 83. https://doi.org/10.1126/science.1143254
12 P. D. Mitcheson, T. C. Green, E. M. Yeatman, and A. S. Holmes: J. Microelectromech. Syst. **13** (2004) 429. https://doi.org/10.1109/JMEMS.2004.830151
13 S. S. Mohan, M. del Mar Hershenson, S. P. Boyd, and T. H. Lee: IEEE J. Solid-State Circuits (1999) 1419. https://doi.org/10.1109/4.792620
14 D. J. Griffiths: Introduction to Electrodynamics (Cambridge University Press: Cambridge, New York, 2018) 4th ed., Chap. 5.

15 I. Khan, M. I. Qureshi, U. U. Rehman, and W. T. Khan: Proc. 2017 Progress in Electromagnetics Research Symp. (PIERS-FALL, 2017) 3079–3085.
16 R. Huang and B. Zhang: IEEE J. Emerg. Sel. Top. Power Electron. **3** (2015) 177. https://doi.org/10.1109/JESTPE.2014.2315997
17 A. P. Sample, D. A. Meyer, and J. R. Smith: IEEE Trans. Ind. Electron. **58** (2011) 544. https://doi.org/10.1109/TIE.2010.2046002
18 H. A. Wheeler: Proc. Inst. Radio Eng. **16** (1928) 1398. https://doi.org/10.1109/JRPROC.1928.221309
19 Y. Yang and C. Wang: Wireless Rechargeable Sensor Networks (Springer Cham, New York, 2015) 1st ed., Chap. 1.

About the Authors

Arvanida Feizal Permana received his B.S. and M.S. degrees from National Chin-Yi University of Technology, Taiwan, in 2020 and 2022, respectively. From 2020 to 2022, he was an assistant researcher at National Chin-Yi University of Technology, Taiwan. His research interests are in wireless power transfer and electronics. (arvanida@gmail.com)

Adhe Martiya received her B.S. degree from National Chin-Yi University of Technology, Taiwan, in 2022 and is currently studying toward her M.S. degree at the same university, Taiwan. Since 2022, she has also been an assistant researcher at National Chin-Yi University of Technology, Taiwan. Her research interests are wireless power transfer, data centers, and electrical power. (adhecha31@gmail.com)

C. Bambang Dwi Kuncoro received his diploma III in electrical engineering from Polytechnic of Bandung Institute of Technology (ITB), Indonesia, in 1993 and his bachelor's and master's degrees in electrical engineering from ITB in 1999 and 2002, respectively. He received his doctoral degree in precision manufacturing from Graduate Institute of Precision Manufacturing, National Chin-Yi University of Technology (NCUT), Taiwan, in 2020. Since 2020, he has been a professor at the Department of Refrigeration, Air Conditioning and Energy Engineering, NCUT. His research interests include sensor integration, embedded systems, control and monitoring applications, wireless sensor networks, wireless power transfer, artificial intelligence, Internet of Things, and renewable energy. (bkuncoro@ncut.edu.tw)

Yean-Der Kuan is a distinguished professor and former chair (2013/02–2019/01) of the Department of Refrigeration, Air Conditioning and Energy Engineering, National Chin-Yi University of Technology, Taichung, Taiwan. He received his Ph.D. degree from the Department of Mechanical and Aerospace Engineering, University of Missouri, USA, in 2000. He is currently the director of the Taiwan Society of Heating, Refrigeration and Air Conditioning, the director of the Taiwan Energy Association, the director of the Taiwan Association for Hydrogen Energy and Fuel Cell, and a member of the American Society of Heating, Refrigerating, and Air-Conditioning. His research interests include energy saving and renewable energies and air-conditioning components and systems. (ydkuan@ncut.edu.tw)